

Highly adaptive principal component regression

Mingxun Wang¹, Alejandro Schuler¹,
Mark van der Laan¹, Carlos García Meixide^{1,2}

¹University of California, Berkeley

²ICMAT, National Research Council of Spain

Abstract

The Highly Adaptive Lasso (HAL) is a nonparametric regression method that achieves almost dimension-free convergence rates under minimal smoothness assumptions, but its implementation can be computationally prohibitive in high dimensions due to the large basis matrix it requires. The Highly Adaptive Ridge (HAR) has been proposed as a scalable alternative. Building on both procedures, we introduce the Principal Component based Highly Adaptive Lasso (PCHAL) and Principal Component based Highly Adaptive Ridge (PCHAR). These estimators constitute an outcome-blind dimension reduction which offer substantial gains in computational efficiency and match the empirical performances of HAL and HAR. We also uncover a striking spectral link between the leading principal components of the HAL/HAR Gram operator and a discrete sinusoidal basis, revealing an explicit Fourier-type structure underlying the PC truncation.

1 Introduction

Adaptive nonparametric regression—methods that automatically adjust to the unknown complexity of the target function—is a cornerstone of modern statistical learning. Classical theory characterizes attainable risk rates under smoothness or structural constraints [Stone, 1982], while modern practice relies on estimators that combine rich function classes with regularization and

data-driven model selection [Donoho and Johnstone, 1994]. A prominent and historically influential route to adaptivity is through spline-based expansions and penalization, including smoothing splines [Wahba, 1990, Green and Silverman, 1994], penalized B-splines (P-splines) [Eilers and Marx, 1996], and locally adaptive regression splines [Mammen and van de Geer, 1997]. Related adaptive basis-selection ideas also appear in multivariate adaptive regression splines (MARS) [Friedman, 1991] and tree-based step-function models such as CART [Breiman et al., 1984]. Stepwise-constant (lower-orthant indicator) basis functions have a long history in nonparametric regression. Early work by [Wong and Shen, 1995] established convergence rates for sieve estimators built from partition-based function classes. Histogram and partitioning estimators were further developed systematically in [Györfi et al., 2002]. Later, [Bühlmann and Yu, 2003] showed that boosting with step functions can yield adaptive estimators in both regression and classification.

In parallel, sparsity-inducing regularization—especially the Lasso [Tibshirani, 1996]—has become a standard mechanism for adaptive selection among a large dictionary of basis functions, with scalable coordinate-descent implementations enabling high-dimensional use in practice [Friedman et al., 2010].

Closely connected “ ℓ_1 -type” nonparametric estimators include total-variation regularization [Rudin et al., 1992], the fused lasso [Tibshirani et al., 2005], and trend filtering [Kim et al., 2009, Tibshirani, 2014], all of which highlight the interplay between rich piecewise-polynomial/step-function representations and convex regularization.

The *Highly Adaptive Lasso* (HAL) [Benkeser and van der Laan, 2016, van der Laan, 2017, van der Laan, 2023, Fang et al., 2021a] is a more recent method for nonparametric regression that has attracted some attention in the literature. HAL constructs a very large linear span of indicator (or, more generally, spline-like) basis functions indexed by axis-aligned knots, and fits the regression via an ℓ_1 -penalized empirical risk minimization [Tibshirani, 1996]. This construction is closely related to the older saturated-spline perspective in which a sufficiently rich basis can interpolate complex shapes while regularization controls complexity [Wahba, 1990, Green and Silverman, 1994, Mammen and van de Geer, 1997, Eilers and Marx, 1996].

A key theoretical feature of HAL is that the ℓ_1 constraint/penalty on the coefficients corresponds to a bounded *sectional variation norm* (a multivariate analogue of bounded variation), which provides an interpretable, low-smoothness complexity measure for high-dimensional regression functions [Benkeser and van der Laan, 2016, van der Laan, 2023]. When the

true regression function has bounded sectional variation norm, the zero-order HAL estimator achieves the convergence rate

$$O_P\left(n^{-1/3}(\log n)^{2(d-1)/3}\right),$$

where the ambient dimension d enters only through a logarithmic factor [Bibaut and van der Laan, 2019, Fang et al., 2021a].

Because of its rate guarantees, HAL has become a convenient nuisance-function learner for semiparametric inference, where the goal is valid estimation and uncertainty quantification for a low-dimensional target parameter in the presence of infinite-dimensional nuisance components. Classical efficiency theory characterizes optimal procedures through tangent spaces and efficient influence functions (EIFs) [Bickel et al., 1993, van der Vaart, 1998, Tsiatis, 2006]. In missing-data and causal-inference settings, foundational work by Robins and collaborators developed inverse-probability-weighted estimating equations and semiparametric efficient procedures, including early doubly-robust constructions [Robins et al., 1994, Robins and Rotnitzky, 1995, Robins et al., 1995]. Targeted Maximum Likelihood Estimation (TMLE) can be viewed as a likelihood-based, plug-in approach that performs a targeted fluctuation step so that the resulting estimator solves (approximately) the EIF estimating equation while allowing flexible machine learning for nuisance estimation [van der Laan and Rubin, 2006, van der Laan and Rose, 2011, van der Laan, 2017]. More recently, Double/Debiased Machine Learning (DML) formalizes closely related principles—Neyman-orthogonal scores and cross-fitting—to enable \sqrt{n} -valid inference when nuisance functions are estimated by high-dimensional or nonparametric learners [Chernozhukov et al., 2018]. All of these methods typically rely on functional nuisance estimates that converge at fast-enough rates in order to remove first-order bias.

Despite these appealing statistical properties, the practical deployment of HAL can be severely limited by computational cost. In its most direct implementation, the HAL design matrix has dimension $n \times p$, where p equals the number of candidate basis functions and can be as large as $p = n(2^d - 1)$ for d covariates. Thus, even when fitting is performed with efficient convex optimization methods for the Lasso [Tibshirani, 1996, Friedman et al., 2010], both (i) constructing the basis/design and (ii) repeatedly solving high-dimensional ℓ_1 -penalized problems (e.g., for cross-validation) can become prohibitive. These difficulties motivate algorithmic reformulations that avoid working directly in the full basis space.

A recent step in this direction is the *Highly Adaptive Ridge* (HAR) estimator [Schuler et al., 2024], which replaces the ℓ_1 penalty in HAL with an ℓ_2 penalty [Hoerl and Kennard, 1970]. Under slightly stricter assumptions, HAR achieves the same convergence rate as HAL. This change enables a kernelized representation: writing the (implicit) HAL feature map as $H \in \mathbb{R}^{n \times p}$ and the associated kernel matrix as $K = HH^\top \in \mathbb{R}^{n \times n}$, the fitted values can be expressed in closed form via the Sherman–Morrison–Woodbury identity [Sherman and Morrison, 1950, Woodbury, 1950]. This viewpoint connects HAR to classical kernel ridge regression and the broader literature on kernel methods [Schölkopf and Smola, 2002, Hastie et al., 2009], while retaining HAL’s data-adaptive feature construction through knots. From a computational perspective, working with K shifts the bottleneck from a potentially enormous p to an $n \times n$ matrix, which is often advantageous when $p \gg n$.

Contribution. In this work, we propose two new estimators—*Principal Components Highly Adaptive Lasso* (PCHAL) and *Principal Components Highly Adaptive Ridge* (PCHAR)—that further reduce the computational cost of HAL/HAR while aiming to preserve predictive performance. Our key idea is to approximate the HAL/HAR kernel matrix K by its leading k principal components, yielding a low-rank representation that projects the regression problem into a k -dimensional orthogonal score space. Low-rank kernel approximations and spectral truncation are classical tools in kernel learning (e.g., kernel PCA and Nyström-type approximations) [Schölkopf et al., 1998, Williams and Seeger, 2001], and scalable randomized algorithms for truncated eigendecompositions/SVD are well developed [Halko et al., 2011]. Our contribution is to bring this spectral perspective *specifically to the HAL/HAR kernel induced by saturated, knot-based features*, and to highlight an *outcome-blind* structure: the embedding is determined entirely by the covariates through their relative feature positions (e.g., coordinatewise order/partial-order relations), not by the response Y . In particular, the eigen-score map can be viewed as a universal, geometry-driven reparameterization of the sample—once the covariates are placed (or sorted, in settings where such a representation applies), the resulting eigen-basis is fixed up to this relative positioning. Exploiting this structure yields estimators with simple analytic forms in the truncated score domain:

- **PCHAR:** an ℓ_2 -penalized estimator that inherits the closed-form ridge solution in the k -dimensional orthogonal basis.

- **PCHAL:** an ℓ_1 -penalized estimator that, due to orthogonality of the retained scores, reduces to *componentwise soft-thresholding* (a direct analogue of the orthogonal-design Lasso solution) [Tibshirani, 1996].

These closed-form solutions eliminate iterative optimization in model fitting and substantially accelerate cross-validation by reducing each refit to (i) a truncated spectral computation and (ii) closed form solutions in \mathbb{R}^k .

Ready-to-use R and Python implementations, including cross-validation routines, are publicly available at <https://github.com/meixide/hapc>.

2 Highly Adaptive Lasso and Ridge

In this section, we summarize the necessary mathematical details of highly adaptive lasso and its estimation procedure. Many of these definitions can also be found in [Owen, 2005, Benkeser and van der Laan, 2016, Schuler et al., 2024].

For a nonempty index set $s \subseteq \{1, \dots, d\}$ and a vector $x = (x_1, \dots, x_d) \in [0, 1]^d$, we write

$$x_s := (x_j)_{j \in s} \in [0, 1]^{|s|}, \quad 0_s := (0, \dots, 0) \in [0, 1]^{|s|}.$$

Given $f : [0, 1]^d \rightarrow \mathbb{R}$, define the s -section (anchored at 0) by

$$f_s : [0, 1]^{|s|} \rightarrow \mathbb{R}, \quad f_s(u_s) := f(u_s, 0_{-s}),$$

where $(u_s, 0_{-s}) \in [0, 1]^d$ denotes the vector whose coordinates in s equal u_s and whose coordinates in the complement $-s := \{1, \dots, d\} \setminus s$ are zero. We also use the rectangle notation

$$(0_s, x_s] := \prod_{j \in s} (0, x_j] \subset (0, 1)^{|s|}.$$

Definition 1. Let $f(x)$ be a function on $[0, 1]^d$. Let $a = (a_1, \dots, a_d)$ and $b = (b_1, \dots, b_d)$ be elements of $[0, 1]^d$ such that $a < b$. A vertex of $[a, b]$ is of the form (c_1, \dots, c_d) where each $c_i \in \{a_i, b_i\}$. Let $\mathcal{V}([a, b])$ be the set of all 2^d vertices of $[a, b]$. We define the sign of a vertex $v = (c_1, \dots, c_d) \in \mathcal{V}([a, b])$ as

$$\text{sign}(v) \equiv (-1)^{\sum_{i=1}^d 1(c_i=a_i)}.$$

That is, the sign of the vertex v is -1 if v contains an odd number of a_i , and 1 if it contains an even number of a_i .

Definition 2. Let $D([0, 1]^d)$ denote the class of functions $f : [0, 1]^d \rightarrow \mathbb{R}$ that are right-continuous with existing left limits in each coordinate (multivariate càdlàg) [Neuhaus, 1971].

Definition 3. The generalized difference of $f \in D([0, 1]^d)$ over an axis-parallel box $A = [a, b] \subset (0, 1]^d$ with vertices $\mathcal{V}(A)$ is defined as

$$\Delta^{(d)}(f; A) \equiv \sum_{v \in \mathcal{V}([a, b])} \text{sign}(v) f(v).$$

For $s = 1, \dots, d$, let

$$0 = x_0^{(s)} < x_1^{(s)} < \dots < x_{m_s}^{(s)} = 1$$

be a partition of $[0, 1]$, and let \mathcal{P} be the partition of $[0, 1]^d$ which is given by

$$\mathcal{P} = \left\{ \left[x_{l_1}^{(1)}, x_{l_1+1}^{(1)} \right] \times \dots \times \left[x_{l_d}^{(d)}, x_{l_d+1}^{(d)} \right] : l_s = 0, \dots, m_s - 1, s = 1, \dots, d \right\}$$

Definition 4. The variation of f on $[0, 1]^d$ in the sense of Vitali is given by

$$V^{(d)}(f; [0, 1]^d) = \sup_{\mathcal{P}} \sum_{A \in \mathcal{P}} |\Delta^{(d)}(f; A)|$$

where the supremum is extended over all partitions of $[0, 1]^d$ into axis-parallel boxes generated by d one-dimensional partitions of $[0, 1]$.

Definition 5. The variation of f on $[0, 1]^d$ in the sense of Hardy and Krause (also called *sectional variation*) is given by

$$\text{Var}_{HK0}(f; [0, 1]^d) = \sum_{\emptyset \neq s \subseteq \{1, \dots, d\}} V^{(|s|)}(f_s; [0, 1]^s)$$

Remark 1. The Hardy-Krause variation anchored at 0 is almost identical to the sectional variation except for the term $f(0)$. We write $V(f)$ to replace $\text{Var}_{HK0}(f; [0, 1]^d)$ to ease the notation.

The following theorem is a key analytical tool underlying the HAL framework, for completeness a proof is given in the appendix; see [Gill et al., 1995, Benkeser and van der Laan, 2016, Van der Laan and Rose, 2018].

Theorem 1 (Sectional Representation of Càdlàg Functions). *Let $f : [0, 1]^d \rightarrow \mathbb{R}$ be a càdlàg function with bounded Hardy–Krause variation anchored at 0, i.e., $V(f) < \infty$. Then f admits the representation*

$$f(x) = f(0) + \sum_{s \neq \emptyset, s \subseteq \{1, \dots, d\}} \int_{(0(s), x(s)]} \mu_{f_s}(du(s)),$$

The proof and the notations are clarified in Appendix 1. Suppose we observe n i.i.d. samples $X_1, \dots, X_n \sim P_0$ taking values in $\mathcal{X} \subseteq [0, 1]^d \subset \mathbb{R}^d$. Our target is an unknown real-valued function

$$f_0 : \mathcal{X} \rightarrow \mathbb{R}$$

assumed to belong to a prespecified function class \mathcal{F} encoding the desired regularity (e.g., smoothness and bounded-variation constraints, such as bounded sectional variation norm). The goal is to estimate f_0 from the data, and we assess an estimator \hat{f} under a prediction loss such as an $L_2(P_0)$ -type criterion. Equivalently, we may view the target as the function-valued parameter

$$\Psi(P_0) = f_0 \in \mathcal{F} \subset \{f : [0, 1] \rightarrow \mathbb{R}\}.$$

The representation in Theorem 1 can be written as

$$f(x) = f(0) + \sum_{\emptyset \neq s \subseteq \{1, \dots, d\}} \int_{0_s}^{1_s} I(u_s \leq x_s) d\mu_{f,s}(u_s). \quad (1)$$

suggesting an underlying regression structure. To connect it to a finite-dimensional estimation problem, we approximate each measure $\mu_{f,s}$ by a discrete signed measure supported on the observed sample. For every nonempty subset $s \subseteq \{1, \dots, d\}$, let $\tilde{x}_{i,s} := (X_i)_s$ denote the projected covariates, adding tilde to indicate the knot points and define

$$\mu_{n,s} = \sum_{i=1}^n \beta_{s,i} \delta_{\tilde{x}_{i,s}},$$

for coefficients $\beta_{s,i} \in \mathbb{R}$. Substituting $\mu_{n,s}$ into (1) yields the finite expansion

$$f_{n,\beta}(x) = f(0) + \sum_{\emptyset \neq s \subseteq \{1, \dots, d\}} \sum_{i=1}^n \beta_{s,i} I(\tilde{x}_{i,s} \leq x_s). \quad (2)$$

Defining basis functions

$$\phi_{s,i}(x) := I(x_s \geq \tilde{x}_{i,s}),$$

we can rewrite (2) as a linear combination of these basis functions. In particular, if we set $\beta_0 := f(0)$, then

$$f_{n,\beta}(x) = \beta_0 + \sum_{\emptyset \neq s \subseteq \{1, \dots, d\}} \sum_{i=1}^n \beta_{s,i} \phi_{s,i}(x). \quad (3)$$

The sectional variation norm of f_n is then given by

$$\|f_{n,\beta}\|_v = |\beta_0| + \sum_{\emptyset \neq s \subseteq \{1, \dots, d\}} \sum_{i=1}^n |\beta_{s,i}|,$$

which mirrors an ℓ_1 -norm on the coefficient vector β .

For estimation, we restrict attention to functions of the form $f_{n,\beta}$ and impose an upper bound on the sectional variation. For a given $M > 0$, define the function classes

$$\mathcal{F}_{n,M} := \left\{ f_{n,\beta} : |\beta_0| + \sum_{\emptyset \neq s \subseteq \{1, \dots, d\}} \sum_{i=1}^n |\beta_{s,i}| \leq M \right\}.$$

We use the empirical risk associated with squared error loss for simplicity

$$\mathcal{R}_n(f) := \frac{1}{n} \sum_{i=1}^n (Y_i - f(X_i))^2.$$

A *HAL estimator* is any minimizer over the sieve:

$$\hat{\beta}_n \in \arg \min_{\beta: f_{n,\beta} \in \mathcal{F}_{n,M}} \mathcal{R}_n(f), \quad \hat{f}_n(x) := f_{\hat{\beta}_n}(x).$$

This optimization problem reduces to a standard penalized regression problem. Let $p := n(2^d - 1)$ denote the total number of non-intercept basis functions, corresponding to the collection $\{\phi_{s,i} : \emptyset \neq s \subseteq \{1, \dots, d\}, i = 1, \dots, n\}$. We define the empirical *HAL design matrix* $H \in \{0, 1\}^{n \times p}$ by

$$H_{j,\ell} := \phi_{s,i}(X_j),$$

where the column index $\ell \in \{1, \dots, p\}$ corresponds to a particular pair (s, i) . Stacking the coefficients $\beta_{s,i}$ into a vector $\beta \in \mathbb{R}^p$, the empirical risk can be viewed as a function of β and the penalty $\|f_\beta\|_v$ becomes an ℓ_1 -type norm on (β_0, β) .

Highly Adaptive Ridge (HAR) is the analogue of HAL obtained by replacing the ℓ_1 -type variation constraint with an ℓ_2 (ridge) penalty on the coefficients. Concretely, HAR uses the same HAL dictionary $\{\phi_{s,i}\}$ and design matrix H , and estimates (β_0, β) by minimizing the empirical mean squared error plus a ridge penalty on β , yielding a ridge-regularized version of the HAL expansion. Unlike HAL, an ℓ_2 penalty does not directly control the Hardy–Krause/sectional variation norm (which corresponds to an ℓ_1 norm of the coefficients in this saturated basis). Consequently, rate guarantees for HAR are typically derived under stronger conditions ensuring effective variation control, e.g., by restricting to (or showing that the oracle approximation lies in) a *shrinking* ℓ_2 -ball such as $\|\beta\|_2 \leq Mn^{-1}$, so that $\|\beta\|_1$ (and hence the sectional variation) remains bounded via Cauchy–Schwarz; see, e.g., Appendix of [Schuler et al., 2024].

3 The Highly Adaptive kernel trick

Now that we have outlined the basic HAL and HAR algorithms, we turn to a discussion of how HAR accelerates the procedure.

Concretely, we define the HAL feature map $h(\cdot)$ to be the vector obtained by evaluating, at a point $x \in [0, \tau]^d$, all lower–orthant indicator monomials $\phi_{i,s}(x)$ indexed by an observation $i \in [n]$ and a nonempty coordinate subset $s \subseteq [d]$. We collect these features into blocks according to the interaction order (equivalently, the number of coordinates involved), namely $k := |s|$. Writing the feature vector as a concatenation of blocks, we have

$$h(x) = (h^{(1)}(x), h^{(2)}(x), \dots, h^{(d)}(x)), \quad h^{(k)}(x) := (\phi_{i,s}(x) : i \in [n], s \subseteq [d], |s| = k).$$

In other words, $h^{(k)}(x)$ consists of all features that depend on exactly k coordinates of x (all k -way interactions). Since there are $\binom{d}{k}$ choices of s with $|s| = k$ and, for each such s , there are n knots indexed by $i \in [n]$, the block $h^{(k)}(x)$ has $n \binom{d}{k}$ entries. Therefore the total number of *non-intercept*

features is

$$p = \sum_{k=1}^d n \binom{d}{k} = n(2^d - 1).$$

An intercept, if desired, can be included separately as an additional constant feature.

The empirical design matrix $H \in \{0, 1\}^{n \times p}$ is obtained by evaluating the dictionary at each training point: the ath row is $h(x_i)^\top$, $i = 1, \dots, n$. We define the associated Gram (kernel) matrix

$$K := HH^\top \in \mathbb{R}^{n \times n}, \quad K_{ij} = h(x_i)^\top h(x_j) =: K(x_i, x_j).$$

Since K is symmetric positive semidefinite, it admits an eigendecomposition $K = UDU^\top$, with U orthogonal and $D = \text{diag}(d_1, \dots, d_n)$ satisfying $d_1 \geq \dots \geq d_n \geq 0$.

A direct expansion gives, for generic $x, x' \in [0, \tau]^d$,

$$\begin{aligned} K(x, x') &= \sum_{i=1}^n \sum_{\emptyset \neq s \subseteq [d]} \mathbf{1}\{x_s \geq \tilde{x}_{i,s}\} \mathbf{1}\{x'_s \geq \tilde{x}_{i,s}\} \\ &= \sum_{i=1}^n \sum_{\emptyset \neq s \subseteq [d]} \mathbf{1}\{(x \wedge x')_s \geq \tilde{x}_{i,s}\}, \end{aligned}$$

where $x \wedge x'$ denotes the componentwise minimum. For each i , define the set of *active coordinates* at the pair of points (x, x')

$$S_i(x, x') := \{j \in [d] : (x \wedge x')_j \geq \tilde{x}_{i,\{j\}}\} = \{j \in [d] : (x \wedge x')_j \geq x_{i,j}\}.$$

Then the inner sum counts the nonempty subsets of $S_i(x, x')$, yielding

$$K(x, x') = \sum_{i=1}^n (2^{|S_i(x, x')|} - 1),$$

which is the closed-form representation of the entries used in [Schuler et al., 2024] and will serve as a computational building block below.

4 PCHAL and PCHAR

With HAL/HAR and the kernel trick in place, we can now present our estimators, which improve over HAL/HAR computationally and admit closed-form

solutions. We first describe the estimators mechanically before discussing their properties.

Building on top of the kernel trick, let

$$H = UD^{1/2}V^\top$$

be a singular value decomposition, where $U \in \mathbb{R}^{n \times n}$ and $V \in \mathbb{R}^{p \times n}$ have orthonormal columns and $D = \text{diag}(d_1, \dots, d_n)$ with $d_1 \geq \dots \geq d_n \geq 0$. For $k \leq n$, let U_k and V_k denote the first k columns of U and V , and let D_k be the leading $k \times k$ principal block of D . We define the *PC score matrix*

$$Z_k := HV_k = U_k D_k^{1/2} \in \mathbb{R}^{n \times k}.$$

Since $K = HH^\top = UDU^\top$, the same U and D appear in the eigendecomposition of K , so Z_k can be computed from K without explicitly forming H or V . Training in PC space then amounts to regressing Y on Z_k with either an ℓ_2 penalty (PCHAR) or an ℓ_1 penalty (PCHAL), yielding well-conditioned optimization in k dimensions while preserving the geometry encoded by K .

Note that

$$Z_k^\top Z_k = D_k^{1/2} U_k^\top U_k D_k^{1/2} = D_k. \quad (4)$$

All optimization is performed with the empirical least-squares loss

$$L(Y, \beta) = \frac{1}{2} \|Y - Z_k \beta\|_2^2.$$

Theorem 2 (PCHA closed forms). *For $\lambda > 0$:*

- *The ridge estimator*

$$\hat{\beta}_{k,\lambda}^{\text{PCHAR}} := \arg \min_{\beta \in \mathbb{R}^k} \left\{ \frac{1}{2n} \|Y - Z_k \beta\|_2^2 + \frac{\lambda}{2} \|\beta\|_2^2 \right\}$$

admits the closed form

$$\hat{\beta}_{k,\lambda}^{\text{PCHAR}} = (D_k + n\lambda I_k)^{-1} D_k^{1/2} U_k^\top Y.$$

- *The lasso estimator*

$$\hat{\beta}_{k,\lambda}^{\text{PCHAL}} := \arg \min_{\beta \in \mathbb{R}^k} \left\{ \frac{1}{2n} \|Y - Z_k \beta\|_2^2 + \lambda \|\beta\|_1 \right\}$$

admits the closed form

$$\hat{\beta}_{k,\lambda}^{\text{PCHAL}} = D_k^{-1} \text{sign}(Z_k^\top Y) \left(|Z_k^\top Y| - n\lambda \right)_+,$$

for coordinates with $d_j > 0$; coordinates with $d_j = 0$ are set to zero.

Tuning For clarity, we develop the theory for fixed (k, λ) , whereas in practice both tuning parameters are chosen data-adaptively by cross-validation. Concretely, we consider a candidate set $k \in \{1, \dots, n\}$ (spacing can be altered). For each fixed k , we run V -fold cross-validation over a small grid of λ values. Let

$$\widehat{\beta}_{k,\lambda}^{(-v)} \in \arg \min_{\beta} \left\{ \frac{1}{2} \|Y^{(-v)} - Z_k^{(-v)} \beta\|_2^2 + \lambda \text{Pen}(\beta) \right\}$$

denote the estimator trained on the data excluding fold v , where $\text{Pen}(\beta) = \|\beta\|_1$ for PCHAL and $\text{Pen}(\beta) = \|\beta\|_2^2$ for PCHAR. We define the cross-validated risk by

$$\text{CVRisk}(k, \lambda) := \frac{1}{V} \sum_{v=1}^V \frac{1}{|I_v|} \|Y^{(v)} - Z_k^{(v)} \widehat{\beta}_{k,\lambda}^{(-v)}\|_2^2,$$

where $(Y^{(v)}, Z_k^{(v)})$ denotes the held-out response vector and PC score matrix on fold v . We then select

$$\hat{\lambda}(k) \in \arg \min_{\lambda} \text{CVRisk}(k, \lambda).$$

Next, we refit on the full sample at $(k, \hat{\lambda}(k))$ to obtain $\widehat{\beta}_{k,\hat{\lambda}(k)}$ and compute the corresponding training mean squared error

$$\text{MSE}_{\text{train}}(k) := \frac{1}{n} \|Y - Z_k \widehat{\beta}_{k,\hat{\lambda}(k)}\|_2^2.$$

Finally, we choose

$$\hat{k} \in \arg \min_{k \in \{1, \dots, n\}} \text{MSE}_{\text{train}}(k), \quad \hat{\lambda} := \hat{\lambda}(\hat{k}),$$

The corresponding refitted PCHAL/PCHAR fitted regression functions are

$$\widehat{f}_{\hat{k},\hat{\lambda}}^{\text{PCHAL}} := Z_{\hat{k}} \widehat{\beta}_{\hat{k},\hat{\lambda}}^{\text{PCHAL}}, \quad \widehat{f}_{\hat{k},\hat{\lambda}}^{\text{PCHAR}} := Z_{\hat{k}} \widehat{\beta}_{\hat{k},\hat{\lambda}}^{\text{PCHAR}}.$$

Prediction Prediction in the principal component-based HAL framework is not entirely trivial. Although the estimated function is linear in the PC scores, those scores are defined through the SVD of the high-dimensional

HAL design matrix $H \in \mathbb{R}^{n \times p}$ with $p = n(2^d - 1)$. Given a fresh sample X'_1, \dots, X'_N , the naive approach would form the expanded design matrix

$$H' = \begin{pmatrix} h(X'_1)^\top \\ \vdots \\ h(X'_N)^\top \end{pmatrix} \in \mathbb{R}^{N \times p}, \quad \text{and compute} \quad f' = H'V_k\hat{\beta},$$

where $V_k \in \mathbb{R}^{p \times k}$ contains the leading k right singular vectors of the training design matrix and $\hat{\beta} \in \mathbb{R}^k$ are the estimated PC coefficients. This is infeasible when p is exponential in d , since neither H' nor V_k can be explicitly stored.

To obtain a computable prediction map, notice that from the SVD of the training design we have

$$V = H^\top U D^{-1/2}.$$

Therefore, for the leading k components,

$$H'V_k = H'H^\top U_k D_k^{-1/2}.$$

Define the *cross-kernel* matrix

$$K' := H'H^\top \in \mathbb{R}^{N \times n},$$

whose (a, b) entry is the inner product $K'(X'_a, X_b) = h(X'_a)^\top h(X_b)$. Then

$$H'V_k = K'U_k D_k^{-1/2}, \quad \text{and hence} \quad f' = (K'U_k D_k^{-1/2})\hat{\beta}.$$

Thus, prediction reduces to computing the new kernel matrix K' in the same closed form as the training Gram matrix $K = HH^\top$, entirely avoiding explicit construction of the high-dimensional objects H' , V_k , or $h(x)$ in \mathbb{R}^p . In practice, we do not penalize the intercept. Accounting for this choice introduces additional centering operations and complicates the notation; we therefore defer the precise formulation in terms of the centered design/kernel matrices (i.e., \tilde{H} and \tilde{K}) to the Appendix E.

An alternative expression, obtained by reparametrizing in the orthonormal basis U_k , is

$$\hat{\beta}_{k,\lambda}^{\text{PCHAL}} = D_k^{-1/2} \text{sign}(U_k^\top Y) (|U_k^\top Y| - \lambda n D_k^{-1/2} \mathbf{1}_k)_+,$$

where $\mathbf{1}_k$ is the k -vector of ones and the absolute value and $(\cdot)_+$ act componentwise. In particular, for each $j \in \{1, \dots, k\}$,

$$\hat{\beta}_{k,\lambda}^{\text{PCHAL}}(j) \neq 0 \iff \lambda < \frac{\sqrt{d_j}}{n} |u_j^\top Y|,$$

where u_j is the j -th eigenvector of K . Thus a cross-validation procedure indexed by λ automatically selects the effective rank: defining

$$W_j := \frac{\sqrt{d_j}}{n} |u_j^\top Y|,$$

the active principal components for a given λ are exactly

$$\{j : W_j > \lambda\}.$$

Sorting the values W_j in decreasing order yields a nested sequence of models in which the number of selected components is monotonically decreasing in λ , in contrast to the standard lasso with correlated features.

4.1 Eigenspace of the Matrix

To get a better understanding of the PC scores, we try to explore the exact eigenspace of the matrix K .

When $d = 1$, the construction becomes deterministic once the sample is sorted. Let $x_{(1)} \leq \dots \leq x_{(n)}$ denote the order statistics. Constructing the HAL design matrix in this ordered basis yields

$$H_{ij} = \mathbf{1}\{x_{(i)} \geq x_{(j)}\} = \mathbf{1}\{i \geq j\}, \quad 1 \leq i, j \leq n,$$

so H is a unit lower-triangular matrix of ones. Its Gram matrix satisfies

$$(HH^\top)_{ij} = \sum_{k=1}^n H_{ik} H_{jk} = \sum_{k=1}^{\min(i,j)} 1 = \min(i, j), \quad 1 \leq i, j \leq n.$$

Consequently,

$$H = \begin{pmatrix} 1 & 0 & 0 & \dots & 0 \\ 1 & 1 & 0 & \dots & 0 \\ 1 & 1 & 1 & \dots & 0 \\ \vdots & \vdots & \vdots & \ddots & \vdots \\ 1 & 1 & 1 & \dots & 1 \end{pmatrix} \quad HH^\top = \begin{pmatrix} 1 & 1 & 1 & \dots & 1 \\ 1 & 2 & 2 & \dots & 2 \\ 1 & 2 & 3 & \dots & 3 \\ \vdots & \vdots & \vdots & \ddots & \vdots \\ 1 & 2 & 3 & \dots & n \end{pmatrix}.$$

In dimensions $d > 1$, an explicit description of the eigenvectors of the zero-order HAL Gram matrix is generally unavailable. The following theorem identifies a tractable special case: when the sample can be totally ordered under the coordinatewise partial order.

Theorem 3 (Eigenstructure of the zero-order HAL Gram matrix). *Assume there exists a permutation π of $\{1, \dots, n\}$ such that, for the reordered sample $X_{(i)} := X_{\pi(i)}$, each coordinate is strictly increasing in i :*

$$X_{(1),j} < X_{(2),j} < \dots < X_{(n),j}, \quad j = 1, \dots, d.$$

Let H be the zero-order indicator HAL design matrix built from all lower-orthant monomials indexed by nonempty coordinate subsets (no intercept), evaluated at $X_{(1)}, \dots, X_{(n)}$, and let $K := HH^\top \in \mathbb{R}^{n \times n}$ be the associated Gram matrix. Then

$$K = (2^d - 1)A, \quad A_{ij} = \min(i, j), \quad 1 \leq i, j \leq n.$$

Equivalently, in the original indexing,

$$K = P^\top((2^d - 1)A)P,$$

where P is the permutation matrix corresponding to π .

Consequently, the eigenvectors of K are obtained by permuting those of A . In particular, an orthonormal eigenbasis of A is given by the discrete sine vectors

$$u_k(i) = \sqrt{\frac{4}{2n+1}} \sin\left(\frac{(2k-1)i\pi}{2n+1}\right), \quad k = 1, \dots, n, \quad i = 1, \dots, n,$$

with eigenvalues

$$\lambda_k(A) = \frac{1}{2\left(1 - \cos\left(\frac{(2k-1)\pi}{2n+1}\right)\right)} = \frac{1}{4\sin^2\left(\frac{(2k-1)\pi}{4n+2}\right)}.$$

Therefore,

$$\lambda_k(K) = (2^d - 1)\lambda_k(A), \quad \text{and} \quad \sigma_k(H) = \sqrt{\lambda_k(K)} = \sqrt{2^d - 1} \frac{1}{2\sin\left(\frac{(2k-1)\pi}{4n+2}\right)}.$$

There is a surprising fact that the eigensystem belong to the covariance matrix of a random walk. A proof of this eigensystem and discussions are given in [Trench, 1999]; for completeness, we include in a self-contained derivation in Appendix 3. Figure 1 overlays the leading eigenvectors of HH^\top with their closed-form discrete sine eigenfunctions.

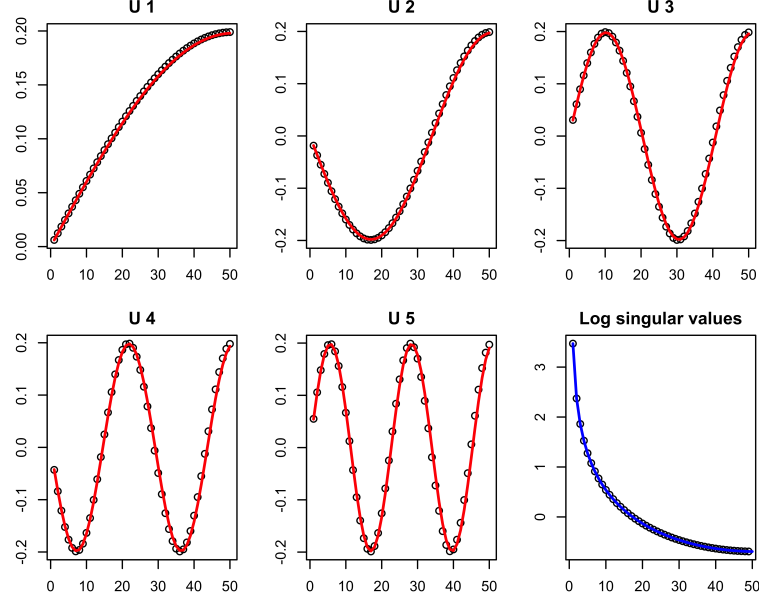


Figure 1: First six eigenvectors of HH^\top (black) if there is a total order, overlaid with their closed-form discrete sine eigenfunctions (red).

5 Controlling interaction order and oracle risk

As hinted in the formula of the eigen vectors, instead of explicitly listing the large amount of sections as covariates, the information of dimension get stucked inside the entries of the matrix K . When the number of covariates become extremely high, we might want to control the interaction order, but most of the case it's not a big deal. The kernel trick can be further extended. If we restrict the dictionary to interactions of order at most m ,

$$h_{\leq m}(x) := (h^{(1)}(x), \dots, h^{(m)}(x)), \quad K_{\leq m}(x, x') := h_{\leq m}(x)^\top h_{\leq m}(x'),$$

then for each i the number of retained subsets is $\sum_{\ell=1}^m \binom{|S_i(x, x')|}{\ell}$, so

$$K_{\leq m}(x, x') = \sum_{i=1}^n \sum_{\ell=1}^m \binom{|S_i(x, x')|}{\ell},$$

as derived in Appendix C.

We consider a collection of estimators indexed by two hyperparameters: a regularization parameter $\lambda \in \Lambda$ and a maximum interaction degree $m \in \{0, 1, \dots, M\}$. For each (m, λ) , we denote by $\hat{f}_{m,\lambda}$ the estimator obtained by fitting PCHA using all basis elements up to interaction degree m , penalized by λ for a fixed rank from 1 to n . The candidate library is therefore the finite set

$$\mathcal{F} = \{\hat{f}_{m,\lambda} : m \in \{0, \dots, M\}, \lambda \in \Lambda\},$$

and we write $K := |\mathcal{F}|$ for its cardinality. Throughout this section we assume that both M and the grid Λ are fixed and do not depend on n , so that K is fixed as $n \rightarrow \infty$.

Under mild regularity conditions, the cross-validation oracle results of [Dudoit and van der Laan, 2005] and [van der Laan et al., 2006] imply that the cross-validated selector performs asymptotically as well, in risk, as the oracle selector that minimizes the true risk over \mathcal{F} . We now make this more precise.

For each candidate model $\hat{f}_{m,\lambda}$, define its theoretical risk under squared error loss as

$$R(m, \lambda) = P_0[(Y - \hat{f}_{m,\lambda}(X))^2],$$

where P_0 denotes the true distribution of (X, Y) . The oracle selector chooses

$$(m^*, \lambda^*) = \arg \min_{m, \lambda} R(m, \lambda),$$

which depends on the unknown P_0 . Cross-validation constructs an empirical estimator $\hat{R}_{\text{CV}}(m, \lambda)$ of $R(m, \lambda)$ using training folds to fit $\hat{f}_{m,\lambda}$ and validation folds to evaluate prediction error. The cross-validated selector is defined by

$$(\hat{m}, \hat{\lambda}) = \arg \min_{m, \lambda} \hat{R}_{\text{CV}}(m, \lambda).$$

A simplified form of the oracle inequalities of [van der Laan et al., 2006] (see also [Dudoit and van der Laan, 2005]) can be written as

$$R(\hat{m}, \hat{\lambda}) - R(m^*, \lambda^*) = O_p\left(\frac{\log K}{n}\right),$$

for bounded loss functions and a fixed validation fraction. In our setting K is fixed, so the remainder is in fact $O_p(n^{-1})$. Thus, cross-validation performs asymptotically as well as the oracle and yields an *oracle approximation* to the minimal risk over \mathcal{F} .

As a concrete illustration, suppose the true regression function has the same aspect as (3) with $d = 3$ and 2-way interactions only. Then, within our library, the oracle chooses $m^* = 2$. If there is a positive gap between the oracle risk $R(m^*, \lambda^*)$ and the risk of all competing models, the $O_p(n^{-1})$ oracle remainder implies that, for large n , cross-validation will also select $\hat{m} = 2$ with probability tending to one. This recovers the usual interpretation: when the model is correctly specified and included in \mathcal{F} , cross-validation behaves like the oracle and selects the correct interaction degree.

5.1 Profiling over the regularization parameter

For each interaction degree m , we define the *profiled* cross-validated risk

$$\hat{R}_{\text{CV}}(m) = \min_{\lambda \in \Lambda} \hat{R}_{\text{CV}}(m, \lambda),$$

where the minimum is taken over the fixed grid of regularization parameters. We then select the interaction degree \hat{m} by

$$\hat{m} = \arg \min_{m \in \{0, \dots, M\}} \hat{R}_{\text{CV}}(m).$$

This profiling strategy is algebraically equivalent to performing cross-validation jointly over all algorithmic candidates:

$$(\hat{m}, \hat{\lambda}) = \arg \min_{(m, \lambda) \in \{0, \dots, M\} \times \Lambda} \hat{R}_{\text{CV}}(m, \lambda).$$

Thus, even though we describe the procedure in two steps (optimize over λ for each fixed m , then over m), the selection rule coincides exactly with the single global minimization over the full candidate library \mathcal{F} .

In practice, this naturally suggests a simple *incremental* or *forward-complexity* search over m : we begin at $m = 1$ and compute $\hat{R}_{\text{CV}}(m)$; if increasing the maximum interaction degree to $m + 1$ does not produce a strictly lower profiled CV risk, then we stop and set $\hat{m} = m$. Formally, the stopping rule is

$$\hat{R}_{\text{CV}}(m + 1) \geq \hat{R}_{\text{CV}}(m) \Rightarrow \hat{m} = m.$$

This argument relies on the fact that all candidate estimators $\hat{f}_{m, \lambda}$ are evaluated using the *same* cross-validation folds, so that the profiled risk curves $\hat{R}_{\text{CV}}(m)$ are directly comparable across m .

If the true regression function does *not* lie in any model with finite interaction degree $m \leq M$, then the oracle index $m^*(n)$ generally depends on n . As n increases, the oracle will gradually favor richer models (larger m), but only to the extent that the variance cost remains controlled. Since cross-validation tracks the oracle at each sample size in the sense of the oracle inequality

$$R(\hat{m}(n), \hat{\lambda}(n)) - R(m^*(n), \lambda^*(n)) = O_p\left(\frac{\log K}{n}\right),$$

it follows that CV adapts to the appropriate complexity at each scale. This is a sample-size-dependent oracle notion: the best interaction degree is itself a function of n , and CV mirrors that adaptivity.

For the PCHAL estimator in particular, the closed-form solution for the lasso path (Theorem 2) shows that increasing λ shrinks and eventually discards principal components according to the threshold statistics

$$W_j := \frac{\sqrt{d_j} |u_j^\top Y|}{n},$$

where d_j is the j -th eigenvalue of $K = HH^\top$ and u_j its corresponding eigenvector. The variance of the j -th principal component is d_j , so W_j combines both variance and alignment with the response Y . As λ increases, principal components drop out in decreasing order of W_j , and the number of distinct active sets along the path is at most $k \leq n$ for each fixed m .

One can therefore view the selection problem as balancing the number of active PCs (at most n) with the maximum interaction degree ($\leq M$), yielding at most

$$K_n \lesssim nM$$

distinct candidate models along the full PC–HAL path. By the adaptive ε -net argument of [van der Laan et al., 2006], cross-validation oracle inequalities continue to hold when the library size K_n grows polynomially with n , with complexity terms of the form

$$\log K_n \lesssim \log n + \log M.$$

In particular, the remainder term in the oracle bound is still of order

$$O_p\left(\frac{\log K_n}{n}\right) = O_p\left(\frac{\log n + \log M}{n}\right),$$

which remains $o_p(1)$ as $n \rightarrow \infty$ for fixed M .

Thus, in finite samples, cross-validation yields a model whose risk is within $O_p(n^{-1})$ of the oracle risk for the given sample size (under a fixed grid Λ), and more generally within $O_p((\log K_n)/n)$ when the library grows at most polynomially. Asymptotically, it adapts to increasing complexity in exactly the same way as the oracle selector.

5.2 Maximum degree of interactions order

The covariates are generated independently as

$$X_{ij} \sim \text{Unif}(-1, 1), \quad i = 1, \dots, n, \quad j = 1, \dots, d,$$

with $d = 3$ throughout. The true regression function contains main effects and second-order interactions:

$$g(X) = \beta^\top X + 0.3(X_1X_2 - 1.5X_2X_3),$$

where $\beta = (1.2, -1.0, 0.8)$, and we generate

$$Y = g(X) + \varepsilon, \quad \varepsilon \sim N(0, 0.03^2).$$

Thus the true model corresponds to maximum interaction order $m_0 = 2$. We consider the candidate library

$$\mathcal{F} = \{\hat{f}_{m,\lambda} : m \in \{1, 2, 3\}, \lambda \in \Lambda\},$$

where Λ is a fixed grid. For each training sample size $n \in \{100, 200, 500\}$, and each $m \in \{1, 2, 3\}$, we compute the cross-validated risk curve

$$\lambda \mapsto \hat{R}_{\text{CV}}(m, \lambda),$$

and record the minimum (profiled) risk

$$\hat{R}_{\text{CV}}(m) = \min_{\lambda \in \Lambda} \hat{R}_{\text{CV}}(m, \lambda).$$

The selected interaction degree is then

$$\hat{m} = \arg \min_{m \in \{1, 2, 3\}} \hat{R}_{\text{CV}}(m).$$

To evaluate oracle performance, we independently generate a fresh test sample of size $n_{\text{test}} = 5000$ and compute the true prediction risk for each (m, λ) . The oracle interaction degree is defined as

$$m^* = \arg \min_{m \in \{1,2,3\}} \min_{\lambda \in \Lambda} R_{\text{test}}(m, \lambda).$$

Table 1 and 2 report, over repeated simulations, the empirical frequencies with which cross-validation selects each m , along with the oracle selection frequencies. The oracle inequality essentially states that these two tables should be similar, in the sense that their behavior differs by a term of order $\mathcal{O}(\frac{1}{n})$. Table 1 illustrates the behavior of the oracle selector, which has access to the full data-generating distribution and can therefore evaluate and minimize the true MSE. As the training sample size increases, the oracle selects models of increasing complexity, since higher interaction orders can be included without incurring overfitting. Table 2 shows the corresponding behavior of the cross-validation (CV) selector, which, as established by the oracle inequality, behaves like the oracle up to an $\mathcal{O}(\frac{1}{n})$ term. Notice that, as the sample size increases, the oracle never selects interaction order 1, as it is not sufficiently expressive for the ground truth; however, for small sample sizes it is selected most of the time, since the oracle deems higher-order interactions overly complex for the available data. The CV selector exhibits the same behavior.

The results illustrate the finite-sample adaptivity behavior predicted by the oracle inequality. When $n = 100$, the signal in the interaction terms is weak relative to sampling variability, and both the oracle and cross-validation frequently prefer $m = 1$, i.e., no interactions. At $n = 200$, the signal-to-noise ratio improves, and both selectors exhibit mixed behavior, allocating non-negligible mass to $m = 2$. Finally, at $n = 500$, the oracle clearly favors $m = 2$, and cross-validation also selects $m = 2$ with high frequency. In other words, as the sample size increases, cross-validation smoothly tracks the oracle transition from preferring simpler main-effects models to preferring interaction models once such structure becomes statistically identifiable.

This matches theoretical arguments: since the candidate library size is fixed, the cross-validated selector performs within $O_p(n^{-1})$ of the oracle risk, and therefore identifies the correct interaction degree once the problem is sufficiently well-conditioned at the available sample size.

Note that we are not working in the of a fully correctly specified finite-dimensional parametric model, where the regression function is exactly a

n	$m = 1$	$m = 2$	$m = 3$
100	0.61	0.24	0.15
300	0.00	0.54	0.46
800	0.00	0.62	0.38

Table 1: Proportion of runs in which each m minimized the oracle MSE.

n	$m = 1$	$m = 2$	$m = 3$
100	0.77	0.18	0.05
300	0.05	0.51	0.44
800	0.00	0.64	0.36

Table 2: Proportion of runs in which each m minimized the cross-validated MSE.

linear combination of products of indicator functions so that the true active set would be contained in our library. In such a setting, the oracle estimator is simply the correctly specified parametric model, and its estimation error converges at the usual parametric rate $n^{-1/2}$. The cross-validation selector would then recover this model, and both the oracle and cross-validated risks would converge at a parametric rate. In our case, however, we are approximating the true regression surface, so the oracle itself depends on the sample size n through the bias–variance tradeoff. Cross-validation tracks this evolving oracle, rather than converging to a fixed finite-dimensional true model.

6 Simulations

6.1 Comparison with ML regressors

For each covariate dimension $d \in \{1, \dots, 10\}$ and sample size $n \in \{200, 400, 600\}$, we generate i.i.d. features $X_1, \dots, X_n \stackrel{\text{i.i.d.}}{\sim} \text{Unif}([0, 1]^d)$ and an independent test set $X_1^{\text{te}}, \dots, X_{n_{\text{te}}}^{\text{te}}$ with $n_{\text{te}} = 2000$ from the same distribution. Responses are $Y_i = g_d(X_i) + \varepsilon_i$, where g_d is a dimension-specific signal defined below and ε_i is mean-zero Gaussian noise with variance calibrated per DGP. Each (d, n) scenario is replicated 5 times. Performance is measured by test MSE, $\frac{1}{n_{\text{te}}} \sum_{i=1}^{n_{\text{te}}} (\hat{g}(X_i^{\text{te}}) - Y_i^{\text{te}})^2$.

6.2 Data-generating processes

We consider dimensions $d \in \{1, \dots, 10\}$ and sample sizes $n \in \{200, 400, 600\}$. For each (d, n) and each DGP g_d , we draw an independent training sample

$\{(X_i, Y_i)\}_{i=1}^n$ and an independent test sample $\{(X_i^{\text{te}}, Y_i^{\text{te}})\}_{i=1}^{n_{\text{test}}}$ with $n_{\text{test}} = 2000$, where $X \sim \text{Unif}([0, 1]^d)$ and $Y = g_d(X) + \varepsilon$ as specified above. Each (d, n) scenario is replicated 5 times. Performance is measured by the test mean squared error

$$\text{MSE} = \frac{1}{n_{\text{test}}} \sum_{i=1}^{n_{\text{test}}} (\hat{g}(X_i^{\text{te}}) - Y_i^{\text{te}})^2,$$

and we report the mean test MSE across the 5 replicates.

$$\mathbf{d1} : \quad g_1(x) = 0.35 x_1 + \sin(2\pi x_1^2) + 0.4 \cos(4\pi x_1) + 0.2 \text{saw}(7x_1) - 0.3 \sigma(12(x_1 - 0.65)), \\ \varepsilon \sim \mathcal{N}(0, 0.05^2).$$

$$\mathbf{d2} : \quad g_2(x) = \sin(\pi x_1 x_2) + 0.5(x_2 - 0.5)^2 + 0.3 \cos(3\pi(x_1 + x_2)) - 0.2 \sin(2\pi(x_1 - x_2)), \\ \varepsilon \sim \mathcal{N}(0, 0.12^2).$$

$$\mathbf{d3} : \quad g_3(x) = 0.6 \sin(2\pi x_1) + 0.6 \cos(2\pi x_2) + 0.6 \sin(2\pi x_3^2) + 0.4 x_2 x_3 \\ + 0.5 \exp(-35\{(x_1 - 0.7)^2 + (x_2 - 0.3)^2 + (x_3 - 0.5)^2\}), \\ \varepsilon \sim \mathcal{N}(0, 0.16^2).$$

$$\mathbf{d4} : \quad g_4(x) = |x_1 - 0.5| + 0.7(x_2 - 0.3)_+ + 0.5|x_3 - 0.7| + 0.6(0.6 - x_4)_+ \\ + 0.3 \mathbf{1}\{x_1 > 0.6\} - 0.25 \mathbf{1}\{x_2 < 0.2\} + 0.2 \mathbf{1}\{x_3 > 0.8, x_4 < 0.4\}, \\ \varepsilon \sim \mathcal{N}(0, 0.18^2).$$

$$\mathbf{d5} : \quad g_5(x) = m^{1.7} + 0.4 \sin(2\pi m) + 0.2(x_1 - 0.5)(x_5 - 0.5), \quad m = \frac{1}{5} \sum_{j=1}^5 x_j, \\ \varepsilon \sim \mathcal{N}(0, 0.16^2).$$

$$\mathbf{d6} : \quad g_6(x) = 1.0 \mathbf{1}\left\{\sum_{j=1}^6 x_j > 3.2\right\} + 0.6 \mathbf{1}\{x_1 > 0.6, x_2 < 0.4\} \\ + 0.4 \mathbf{1}\{x_3 > 0.7, x_4 < 0.3\} + 0.3 \mathbf{1}\{x_5 + x_6 > 1.1\}, \\ \varepsilon \sim \mathcal{N}(0, 0.15^2).$$

$$\mathbf{d7} : \quad g_7(x) = \sum_{j=1}^7 w_j \sin(A_j \pi x_j) + 0.2(x_1 - 0.5)(x_3 - 0.5) - 0.2(x_5 - 0.5)(x_7 - 0.5),$$

$$A_j = \text{linspace}(7, 13), \quad w_j = \text{linspace}(1, 0.4),$$

$$\varepsilon \sim \mathcal{N}(0, 0.20^2).$$

$$\mathbf{d8} : \quad g_8(x) = \exp\left(-30 \sum_{j=1}^8 (x_j - 0.3)^2\right) - 0.8 \exp\left(-30 \sum_{j=1}^8 (x_j - 0.7)^2\right)$$

$$+ 0.3 \sin(2\pi \bar{x}_{1:8}) + 0.2 \cos(2\pi(x_1 + x_8)),$$

$$\varepsilon \sim \mathcal{N}(0, 0.18^2).$$

$$\mathbf{d9} : \quad g_9(x) = 0.8 \sin(\pi x_1 x_2) + 0.25(x_3 - 0.5)(x_9 - 0.5) + 0.3x_7 x_8 + 0.6 \cos(2\pi \bar{x}_{1:9}),$$

$$\varepsilon \sim \mathcal{N}\left(0, [0.10 + 0.30 \cdot \overline{(x_{1:9}^2)}]^2\right) \quad (\text{heteroskedastic}).$$

$$\mathbf{d10} : \quad g_{10}(x) = g_1 + 0.6 g_2 + g_3,$$

$$g_1 = \left(\sum_{\ell=1}^4 \lfloor 3x_\ell \rfloor \right) \bmod 2 - \frac{1}{2}, \quad g_2 = \frac{1}{10} \sum_{j=1}^{10} \cos(2\pi j x_j),$$

$$g_3 = 0.2(x_5 - 0.6)_+ + 0.2(0.4 - x_6)_+ + 0.2 \mathbf{1}\{x_9 > 0.75\},$$

$$\varepsilon \sim \mathcal{N}(0, 0.18^2).$$

6.3 HAL design and HAL-family estimators

All methods that consume a HAL design use the zero-order (pure indicator) HAL basis of [Benkeser and van der Laan, 2016]. For a given dimension d and covariate matrix $X \in [0, 1]^{n \times d}$, we enumerate the HAL basis with `max_degree = d`, `smoothness_orders` all zero, and `include_lower_order` set to `TRUE`. The corresponding design matrix uses `p_reserve = 0`, so there are no unpenalized raw-coordinate columns; the basis is a pure collection of indicator functions of axis-aligned rectangles.

We consider the following HAL-family estimators:

- **PCHAL / PCHAR** (principal-component HAL): given the HAL design $H \in \mathbb{R}^{n \times p}$, we compute its empirical principal components and fit penalized least-squares models in the PC coordinates. For both PCHAL and PCHAR we use the same grid of candidate PC dimensions $k \in \mathcal{K}$ (bounded by the numerical rank). For each $k \in \mathcal{K}$, a

5-fold cross-validation selects the regularization parameter λ on a log-scale grid $\log_{10} \lambda \in [-9, 1]$ with 25 equally spaced values. We then select k by minimizing the resulting *training* MSE over the candidate set. Finally, at the selected k , we refit and again choose λ by 5-fold cross-validation on the same grid. PCHAL uses an ℓ_1 penalty in the PC coordinates, while PCHAR uses an ℓ_2 penalty. The response is centered prior to fitting and the features are centered prior to PCA.

- **HAL**: ℓ_1 -penalized least-squares on the HAL design H , fitted via `glmnet` with 10-fold cross-validation, `lambda.min.ratio` = 10^{-6} , and `nlambda` = 250.
- **HAR**: ℓ_2 -penalized least-squares on the HAL design with an explicit unpenalized intercept. We augment H with a column of ones and pass penalty factor 0 for the intercept and 1 for all other columns. The same 10-fold CV and λ grid as for HAL are used.

6.4 Baselines and hyperparameters

We compare the HAL family against widely-used nonparametric regressors. All baselines are tuned using compact but robust hyperparameter grids.

- **k -nearest neighbors** (kNN): candidate neighborhood sizes scale with n via

$$k \in \text{unique}\left(\text{round}\left\{\sqrt{n}/2, \sqrt{n}, 2\sqrt{n}, n^{2/3}/3, n^{2/3}\right\}\right),$$

truncated to integers satisfying $2 \leq k < n$, and k is chosen by 5-fold CV.

- **Random forest** (RF): implemented with `ranger`. We fix `num.trees` = 800, set `mtry` = 1 when $d = 1$ and `mtry` = $\lceil \sqrt{d} \rceil$ otherwise, use `sample.fraction` = 0.632, and `min.node.size` = $\max\{5, \lfloor n/200 \rfloor\}$.
- **XGBoost**: gradient-boosted trees with histogram splitting and early stopping. We perform 5-fold CV over the grid $\eta \in \{0.05, 0.10, 0.20\}$, `max_depth` $\in \{3, 5, 7\}$, and `min_child_weight` $\in \{1, 5\}$, with subsampling and column subsampling fixed at 0.8. For each grid point we run up to 1200 rounds with a patience of 60 for early stopping, selecting the configuration and number of rounds that minimize the CV RMSE.

- **Kernel ridge regression** (KRR): we use a Gaussian RBF kernel. Let \hat{m} denote the median of squared pairwise distances $\|X_i - X_j\|^2$ computed on the training set. We consider kernel parameters

$$\sigma \in \{0.25, 0.5, 1, 2, 4\}/\hat{m} \quad \text{and} \quad \lambda \in 10^{\{-6, -5, -4, -3, -2, -1\}},$$

and select (λ, σ) by 5-fold cross-validation. With the selected pair, we fit KRR by solving

$$(K + n\lambda I)\alpha = Y,$$

and predict using the corresponding cross-kernel between test and training points.

- **Generalized additive model** (GAM): we fit a model of the form $Y \sim \sum_{j=1}^d s(X_j, k)$ using `mgcv`, where the basis dimension is $k = \min\{60, \max(10, \lfloor n/5 \rfloor)\}$ and smoothing parameters are estimated by REML.
- **Multivariate adaptive regression splines** (MARS): implemented via `earth`. For $d = 1$ we restrict to degree 1; otherwise we consider degree $\in \{1, 2\}$. The maximum number of terms `nk` is gridded between $\lfloor 0.10n \rfloor$ and $\lfloor 0.85n \rfloor$ (10 equally spaced values). We use `pmethod = backward` pruning with penalty $\in \{1, 1.2, 1.5, 2, 3\}$, and select (degree, `nk`, penalty) by 5-fold CV.

6.5 Training and evaluation

We consider dimensions $d \in \{1, \dots, 10\}$ with sample sizes $n \in \{200, 400, 600\}$. For each (d, n) and each DGP g_d we draw an independent training sample of size n and an independent test sample of size $n_{\text{test}} = 2000$ from the same distribution $X \sim \text{Unif}([0, 1]^d)$, and generate responses as described above. We repeat each scenario for 5 Monte Carlo replicates and report the mean test mean squared error (MSE) across replicates.

Table 3: Averaged MSE

	$d = 1$	$d = 2$	$d = 3$	$d = 4$	$d = 5$	$d = 6$	$d = 7$	$d = 8$	$d = 9$	$d = 10$
	$n = 200$									
pchal	0.005	0.065	0.039	0.044	0.032	0.157	1.877	0.057	0.072	0.570
pchar	0.006	0.053	0.039	0.042	0.032	0.153	1.914	0.056	0.068	0.589
hal (lasso)	0.006	0.057	0.043	0.045	0.033	0.172	1.980	0.056	0.071	0.596
hal (ridge)	0.005	0.055	0.038	0.042	0.031	0.151	1.950	0.055	0.067	0.572
xgb	0.006	0.119	0.046	0.046	0.032	0.162	1.895	0.056	0.072	0.596
knn	0.005	0.028	0.092	0.061	0.031	0.160	1.922	0.060	0.084	0.573
rf	0.004	0.044	0.084	0.052	0.032	0.170	1.848	0.057	0.073	0.569
krr	0.003	0.019	0.043	0.048	0.031	0.134	1.855	0.054	0.067	0.549
gam	0.003	0.103	0.032	0.040	0.031	0.158	1.958	0.057	0.078	0.583
mars	0.005	0.049	0.037	0.042	0.036	0.174	2.063	0.067	0.081	0.590
	$d = 1$	$d = 2$	$d = 3$	$d = 4$	$d = 5$	$d = 6$	$d = 7$	$d = 8$	$d = 9$	$d = 10$
	$n = 400$									
pchal	0.003	0.034	0.033	0.040	0.031	0.135	1.900	0.054	0.065	0.261
pchar	0.003	0.033	0.033	0.040	0.030	0.129	1.915	0.052	0.060	0.286
hal (lasso)	0.004	0.035	0.036	0.040	0.031	0.141	1.854	0.051	0.062	0.257
hal (ridge)	0.003	0.033	0.033	0.040	0.030	0.129	1.897	0.051	0.059	0.261
xgb	0.004	0.108	0.039	0.042	0.032	0.141	1.848	0.052	0.064	0.259
knn	0.003	0.022	0.073	0.057	0.030	0.134	1.926	0.054	0.078	0.264
rf	0.003	0.028	0.064	0.047	0.031	0.144	1.858	0.052	0.068	0.259
krr	0.003	0.016	0.034	0.047	0.029	0.118	1.903	0.051	0.059	0.261
gam	0.003	0.099	0.029	0.039	0.031	0.152	1.921	0.054	0.074	0.263
mars	0.004	0.031	0.032	0.038	0.032	0.165	1.990	0.055	0.072	0.266
	$d = 1$	$d = 2$	$d = 3$	$d = 4$	$d = 5$	$d = 6$	$d = 7$	$d = 8$	$d = 9$	$d = 10$
	$n = 600$									
pchal	0.003	0.026	0.031	0.038	0.029	0.127	1.850	0.053	0.062	0.363
pchar	0.003	0.026	0.031	0.038	0.030	0.122	1.850	0.051	0.058	0.384
hal (lasso)	0.003	0.026	0.034	0.038	0.030	0.126	1.792	0.049	0.061	0.361
hal (ridge)	0.003	0.026	0.031	0.038	0.029	0.122	1.834	0.051	0.057	0.360
xgb	0.003	0.108	0.036	0.039	0.030	0.129	1.764	0.050	0.062	0.377
knn	0.003	0.020	0.060	0.050	0.029	0.126	1.875	0.054	0.073	0.348
rf	0.003	0.023	0.054	0.044	0.029	0.132	1.793	0.053	0.065	0.356
krr	0.002	0.015	0.032	0.045	0.028	0.110	1.862	0.053	0.055	0.361
gam	0.003	0.101	0.030	0.037	0.030	0.153	1.854	0.054	0.075	0.363
mars	0.004	0.026	0.032	0.037	0.030	0.144	1.872	0.052	0.067	0.367

Across the 30 benchmark scenarios (ten DGPs with $d = 1, \dots, 10$ and $n \in \{200, 400, 600\}$), the most consistent takeaway from the MSE tables is that the PC-based HAL estimators deliver *near-HAR* predictive accuracy while remaining competitive with the best classical HAL fit. In particular, **PCHAR** tracks HAR extremely closely across essentially all dimensions: averaged over the 30 (n, d) settings, its test MSE is only about 1–2% higher than HAR, and in the tables the two are often indistinguishable at three-decimal

precision (indeed, in 24/30 settings the absolute gap is at most 0.005). Moreover, PCHAR is *slightly better than* HAL on average (about a 3% reduction in MSE across the 30 settings), and it improves upon HAL in a majority of the table entries (17 out of 30).

The ℓ_1 variant **PCHAL** is somewhat more variable than PCHAR but remains a strong performer overall. Relative to HAR, its MSE is typically within a few percent, and it is frequently tied for the best result within the HAL-family (PCHAL is the smallest HAL-family entry in 11 of the 30 settings, mostly via near-ties). Importantly, PCHAL can be *strictly* better than the other HAL-type fits in some of the harder designs: for example, in the $d = 7$ DGP at $n = 200$, PCHAL attains 1.877 versus 1.914 (PCHAR), 1.980 (HAL), and 1.950 (HAR). This pattern is consistent with PCHAL occasionally benefiting from sparsity in the PC coordinates on more irregular signals, even though PCHAR is slightly more reliable on average.

Among the baselines, **KRR** is the clearest accuracy leader in many columns, and in several scenarios the gap is substantial. This is most visible in the interaction-heavy $d = 2$ setting, where KRR achieves 0.019/0.016/0.015 for $n = 200/400/600$, compared to roughly 0.053/0.033/0.026 for PCHAR (and 0.065/0.034/0.026 for PCHAL). A similar advantage appears in the thresholded indicator-style $d = 6$ setting (e.g., 0.134/0.118/0.110 for KRR versus 0.153/0.129/0.122 for PCHAR). That said, outside these KRR-favorable regimes, the PC-HAL methods are typically close to the best-performing procedures and compare favorably to more specialized learners that have clear failure modes (e.g., the additive GAM is markedly worse on the non-additive $d = 2$ design). KRR's strong performance here is plausibly tied to the fact that many of the DGPs are predominantly smooth (trigonometric components, low-order interactions, and localized Gaussian bumps), which aligns well with the smoothness bias of an RBF kernel when the bandwidth is tuned. This advantage is therefore highly DGP-dependent: if the signal were substantially less smooth (e.g., dominated by sharper thresholding or more discontinuous structure), KRR could lose ground, whereas HAL-type indicator bases are designed to represent such nonsmooth features more directly.

Overall, the MSE tables support the following honest summary: HAR remains a strong accuracy benchmark; PCHAR is an excellent surrogate that essentially preserves HAR accuracy and is often slightly better than HAL; and PCHAL is a competitive alternative that is usually close to PCHAR and can sometimes be the best HAL-type method on the more irregular designs. Meanwhile, KRR is the strongest generic baseline and frequently the overall

winner, but PCHAL/PCHAR remain attractive when one wants a HAL-style representation while maintaining consistently strong predictive performance across a wide range of signal structures.

7 Real-data benchmark

We further evaluate the same set of learners and tuning strategies used in the simulation study on a collection of real-world regression datasets [Dua et al., 2017]. For each dataset, we retain up to $N_{\max} = 2000$ complete observations (dropping rows with missing values). Within each repetition, we split the data into an 80%/20% train/test partition, apply train-fitted min-max scaling to map each feature to $[0, 1]$, and evaluate predictive accuracy by test RMSE. Results are averaged over $R = 5$ random splits.

Table 4 reports mean test RMSE for each dataset (best method per row in bold). A clear pattern is that the PC-based HA estimators (PCHAR/PCHAL) behave *stably* across datasets: they are rarely the very best method, but they also avoid severe degradations and typically remain close to the full HA-kernel benchmark (e.g., the three HA variants are essentially indistinguishable on `yearmsd`). In contrast, several competing learners exhibit more pronounced dataset-to-dataset variability: they can achieve the lowest RMSE on some problems (e.g., tree/boosting methods on `blog`, `energy`, `power`, `wine`, `yacht`, `yearmsd`) yet perform noticeably worse on others (e.g., RKRR is excellent on `kin8nm` but substantially worse on `blog/yearmsd`). Similarly, strongly structured models can be highly competitive when their assumptions align with the data (e.g., GAM on `naval`) but less so elsewhere. A small number of entries are omitted on very wide datasets due to practical runtime constraints and are shown as missing in the table.

data	n	p	HAR	PCHAR	PCHAL	RKRR	RF	Ridge	kNN	GAM	MARS	XGB
blog	2000	266	7.72	7.73	8.50	1.23e+1	1.69e+1	2.08e+1	—	—	—	6.82
boston	506	13	3.53	3.53	3.68	3.20	3.33	4.85	5.48	3.67	3.74	3.10
concrete	1030	8	3.82	4.83	3.90	5.53	5.34	1.04e+1	9.85	5.39	5.25	4.06
energy	768	8	3.75e-1	3.97e-1	3.91e-1	6.26e-1	8.11e-1	2.87	2.59	1.04	4.86e-1	2.98e-1
kin8nm	2000	8	1.41e-1	1.41e-1	1.50e-1	9.06e-2	1.73e-1	2.01e-1	1.47e-1	1.98e-1	1.76e-1	1.46e-1
naval	2000	15	8.98e-4	8.96e-4	1.05e-3	7.36e-4	1.21e-3	4.48e-3	6.67e-3	2.59e-5	4.55e-4	8.10e-4
power	2000	4	4.03	4.21	4.09	4.27	4.02	4.58	4.47	4.21	4.31	3.90
protein	2000	9	1.81	1.84	1.81	2.08	1.79	2.30	2.15	1.85	1.85	1.87
wine	1599	11	6.11e-1	6.11e-1	6.42e-1	6.42e-1	5.94e-1	6.60e-1	6.70e-1	6.51e-1	6.62e-1	5.91e-1
yacht	308	6	7.28e-1	7.28e-1	7.35e-1	8.06e-1	2.08	8.34	9.19	1.69	1.15	5.38e-1
yearmsd	2000	90	1.16e+1	1.16e+1	1.16e+1	9.21e+1	1.01e+1	1.01e+1	—	—	—	9.23

Table 4: Real Dataset Mean RMSE

A Proof of Theorem 1

The proof is a slight modification of [Fang et al., 2021b].

Definition 6. A function f on $[0, 1]^d$ is called **completely monotone** [Aistleitner and Dick, 2014] if for any closed axis-parallel box $A \subset [0, 1]^d$ of arbitrary dimension s (where $1 \leq s \leq d$), its s -dimensional quasi-volume generated by the function f is non-negative.

Lemma 1. *For $V(f) < \infty$, $f(x) = f_1(x) - f_2(x)$ where $f_1(x)$ and $f_2(x)$ are completely monotone on $[0, 1]^d$.*

This is a multivariate extension of the Jordan decomposition on \mathbb{R} . While any function of bounded variation admits a decomposition into the difference of two completely monotone functions $f = f_1 - f_2$ (Leonov 1996) [Leonov, 1996], a naive choice such as $f_1(x) = \text{Var}_{HK0}(f; [0, x])$ and $f_2(x) = f_1(x) - (f(x) - f(0))$ is generally insufficient for our purposes.

Specifically, in d dimensions, the function f_2 defined this way is not guaranteed to be completely monotone, meaning its quasi-volumes over sub-boxes may be negative. Furthermore, even if f_1 and f_2 were monotone, such a decomposition is generally not **unique** and does not satisfy the property that the total variation of the function equals the sum of the variations of its components. We are interested in the **canonical Jordan decomposition**, which is the unique representation $f = f(0) + f^+ - f^-$ anchored at zero that satisfies the variation identity:

$$V(f) = V(f^+) + V(f^-).$$

This specific decomposition is essential because it ensures a one-to-one correspondence with the Jordan decomposition of the signed measure μ_f . The existence of this representation is established in the following theorem.

Theorem 4. *Let f be a cadlag function on $[0, 1]^d$ with bounded HK variation. Then there exist two uniquely determined completely monotone functions f^+ and f^- on $[0, 1]^d$ such that $f^+(0) = f^-(0) = 0$ and*

$$f(x) = f(0) + f^+(x) - f^-(x), \quad x \in [0, 1]^d,$$

and

$$V(f) = V(f^+) + V(f^-).$$

$$\begin{aligned} f^+(x) &= \frac{1}{2} (\text{Var}_{\text{HK0}}(f; [0, x]) + f(x) - f(0)), \\ f^-(x) &= \frac{1}{2} (\text{Var}_{\text{HK0}}(f; [0, x]) - f(x) + f(0)). \end{aligned}$$

Aistleitner and Dick [Aistleitner and Dick, 2014] proved that the two functions are completely monotone.

Theorem 5. *Let f be a cadlag function on $[0, 1]^d$ with $V(f) < \infty$. Then there exists a unique signed Borel measure μ_f on $[0, 1]^d$ for which*

$$f(x) = \mu_f([0, x]), \quad x \in [0, 1]^d.$$

Then we have

$$\text{Var}_{\text{total}} \mu_f = V(f) + |f(0)|.$$

Notice that $\text{Var}_{\text{total}} \mu_f$ is the total variation of μ_f given by the Jordan decomposition of the measure.

Furthermore, if

$$f(x) = f(0) + f^+(x) - f^-(x)$$

is the Jordan decomposition of f , and $\mu_f = \mu_f^+ - \mu_f^-$ is the Jordan decomposition of μ_f , then

$$f^+(x) = \mu_f^+([0, x] \setminus \{0\}) \quad \text{and} \quad f^-(x) = \mu_f^-([0, x] \setminus \{0\}), \quad x \in [0, 1]^d.$$

The details of the proof can be found in their paper. We start with the set function μ_f^+ on the elements of all closed axis-parallel boxes contained in $[0, 1]^d$ which have one vertex at the origin.

$$\mu_f^+([0, x]) = f^+(x), \quad \text{for } x \in [0, 1]^d.$$

We generate the measure on the Borel sigma algebra by the Carathéodory extension theorem, similarly for μ_f^- . The details can be found in Yeh (2006) [Yeh, 2006] or Bogachev (2007) [Bogachev and Ruas, 2007]. Finally, we define

$$\mu_f = \mu_f^+ - \mu_f^- + \delta_0 f(0).$$

Then μ_f is a finite signed Borel measure, and we have

$$\mu_f([0, x]) = f^+(x) - f^-(x) + f(0) = f(x).$$

Thus the identity is rigorously justified,

$$f(x) = \int_{[0,x]} d\mu_f(u).$$

For the cube $[0, 1]^d$, we define for each subset $s \subset \{1, \dots, d\}$ the edge $E_s \equiv \{(x(s), 0(-s)) : x \in (0, 1]^d\} \subset [0, 1]^d$, where $x(s) \equiv (x(j) : j \in s)$ and $0(-s) = (0(j) : j \notin s)$. For the empty subset $s = \emptyset$, we define $E_s = \{0\} \subset [0, 1]^d$ as the singleton 0. Note that for $s = \{1, \dots, d\}$, we have $E_s = (0, 1]^d$. For any $x \in [0, 1]^d$, consider the d -dimensional interval $[0, x]$. We can partition this interval into disjoint "faces" based on which coordinates are strictly positive. Specifically, we have the disjoint union:

$$[0, x] = \{0\} \cup \bigcup_{\emptyset \neq s \subseteq \{1, \dots, d\}} (E_s \cap [0, x])$$

where $E_s = \{(u(s), 0(-s)) : u(s) \in (0, 1)^{|s|}\}$. For a given x , the intersection $E_s \cap [0, x]$ is non-empty if and only if $x_j > 0$ for all $j \in s$. When non-empty, this set is isometric to the $|s|$ -dimensional half-open interval $(0(s), x(s))$.

Using the identity $f(x) = \mu_f([0, x])$ established above and the finite additivity of the measure μ_f , we obtain:

$$f(x) = \mu_f(\{0\}) + \sum_{\emptyset \neq s \subseteq \{1, \dots, d\}} \mu_f(E_s \cap [0, x])$$

By the definition of the measure at the origin, $\mu_f(\{0\}) = f(0)$. Furthermore, for each non-empty s , we define the sectional measure μ_{f_s} as the restriction of μ_f to the face E_s . Identifying $E_s \cap [0, x]$ with the lower-dimensional interval $(0(s), x(s))$, we can write:

$$\mu_f(E_s \cap [0, x]) = \int_{(0(s), x(s))} \mu_{f_s}(du(s))$$

Summing these contributions yields the desired representation:

$$f(x) = f(0) + \sum_{s \neq \emptyset, s \subseteq \{1, \dots, d\}} \int_{(0(s), x(s))} \mu_{f_s}(du(s))$$

B Proof of Theorem 3

B.1 Eigenstructure of $A_{ij} = \min(i, j)$ via a discrete second-difference problem

Let $L \in \mathbb{R}^{n \times n}$ be the unit lower-triangular matrix

$$L_{ij} = \mathbf{1}\{i \geq j\}.$$

A direct calculation gives

$$A := LL^\top, \quad A_{ij} = \sum_{k=1}^{\min(i,j)} 1 = \min(i, j).$$

The inverse of L is the first-difference operator $D := L^{-1}$ with entries

$$D_{11} = 1, \quad D_{ii} = 1, \quad D_{i,i-1} = -1 \ (i \geq 2), \quad 0 \text{ otherwise.}$$

Hence

$$A^{-1} = L^{-\top} L^{-1} = D^\top D = \begin{bmatrix} 2 & -1 & & & \\ -1 & 2 & -1 & & \\ & \ddots & \ddots & \ddots & \\ & & -1 & 2 & -1 \\ & & & -1 & 1 \end{bmatrix}.$$

Let $x \in \mathbb{R}^n$ and consider the eigenproblem

$$A^{-1}x = \mu x.$$

Componentwise, this is

$$\begin{aligned} 2x_1 - x_2 &= \mu x_1, \\ -x_{r-1} + 2x_r - x_{r+1} &= \mu x_r, \quad r = 2, \dots, n-1, \\ -x_{n-1} + x_n &= \mu x_n. \end{aligned}$$

It is convenient to encode the boundary rows using ghost nodes: define $x_0 := 0$ and enforce $x_{n+1} := x_n$. Then the same interior stencil

$$-x_{r-1} + 2x_r - x_{r+1} = \mu x_r$$

holds for *all* $r = 1, \dots, n$.

Now, we seek solutions of the form $x_r = \sin(r\theta)$. Using $\sin((r+1)\theta) + \sin((r-1)\theta) = 2\cos\theta \sin(r\theta)$, the stencil gives

$$\mu(\theta) = 2(1 - \cos\theta) = 4\sin^2(\theta/2).$$

The boundary condition $x_{n+1} = x_n$ becomes

$$\sin((n+1)\theta) = \sin(n\theta) \iff 2\cos\left(\frac{(2n+1)\theta}{2}\right)\sin\left(\frac{\theta}{2}\right) = 0.$$

For nontrivial eigenvectors we take $\sin(\theta/2) \neq 0$, hence

$$\cos\left(\frac{(2n+1)\theta}{2}\right) = 0 \quad \Rightarrow \quad \theta_k = \frac{(2k-1)\pi}{2n+1}, \quad k = 1, \dots, n.$$

Thus an eigenbasis of A^{-1} is given by

$$x_r^{(k)} = \sin(r\theta_k), \quad \mu_k = 2(1 - \cos\theta_k).$$

Step 4: Convert to eigenpairs of A and normalize. Since $A^{-1}x^{(k)} = \mu_k x^{(k)}$, the eigenvalues of A are

$$\lambda_k(A) = \frac{1}{\mu_k} = \frac{1}{2(1 - \cos\theta_k)} = \frac{1}{4\sin^2(\theta_k/2)}.$$

Moreover, $\sum_{r=1}^n \sin^2(r\theta_k) = \frac{2n+1}{4}$, so the normalized eigenvectors are

$$u_k(r) = \sqrt{\frac{4}{2n+1}} \sin(r\theta_k), \quad r = 1, \dots, n.$$

Therefore $A = U \operatorname{diag}(\lambda_1(A), \dots, \lambda_n(A)) U^\top$ with $U = [u_1 \ \cdots \ u_n]$.

B.2 Continuum limit and Fourier/Sturm–Liouville connection

Let $h := \frac{1}{n+1}$ and $s_i := ih$ for $i = 1, \dots, n$. Then

$$A_{ij} = \min(i, j) = \frac{1}{h} \min(s_i, s_j), \quad \text{equivalently} \quad \min(s_i, s_j) = h A_{ij}.$$

Define the continuum integral operator

$$(Tf)(s) = \int_0^1 \min(s, t) f(t) dt, \quad s \in [0, 1].$$

For a smooth f and the grid vector $f_i := f(s_i)$, the Riemann-sum approximation gives

$$(Tf)(s_i) \approx h \sum_{j=1}^n \min(s_i, s_j) f(s_j) = h \sum_{j=1}^n (h A_{ij}) f_j = h^2 (Af)_i.$$

Thus the *scaled matrix* $h^2 A$ is the natural discretization of T , and the eigenvalues satisfy $h^2 \lambda_k(A) \rightarrow \lambda_k(T)$ as $n \rightarrow \infty$ (for fixed k).

Green's function and Sturm–Liouville operator. The kernel $K_\infty(s, t) = \min(s, t)$ is the Green's function of the self-adjoint operator $-\frac{d^2}{ds^2}$ on $[0, 1]$ with mixed boundary conditions

$$u(0) = 0, \quad u'(1) = 0.$$

Accordingly, the associated Sturm–Liouville eigenproblem is

$$-\phi''(s) = \mu \phi(s) \quad (0 < s < 1), \quad \phi(0) = 0, \quad \phi'(1) = 0. \quad (5)$$

Its eigenpairs are the half-shifted sines

$$\phi_k(s) = \sqrt{2} \sin\left((k + \frac{1}{2})\pi s\right), \quad \mu_k = ((k + \frac{1}{2})\pi)^2, \quad k = 0, 1, 2, \dots,$$

and since T is the inverse of $-\frac{d^2}{ds^2}$ under these boundary conditions,

$$T\phi_k = \lambda_k(T)\phi_k, \quad \lambda_k(T) = \frac{1}{\mu_k} = \frac{1}{((k + \frac{1}{2})\pi)^2}.$$

Matching to the discrete eigensystem. Recall the discrete eigenpairs of A :

$$\theta_k = \frac{(2k - 1)\pi}{2n + 1}, \quad u_k(i) = \sqrt{\frac{4}{2n + 1}} \sin(i\theta_k), \quad \lambda_k(A) = \frac{1}{2(1 - \cos\theta_k)}, \quad k = 1, \dots, n.$$

For fixed k and $n \rightarrow \infty$, we have $\theta_k \sim (k - \frac{1}{2})\pi h$ and hence

$$h^2 \lambda_k(A) = \frac{h^2}{2(1 - \cos\theta_k)} \longrightarrow \frac{1}{((k - \frac{1}{2})\pi)^2} = \lambda_{k-1}(T),$$

while $u_k(i) \approx \phi_{k-1}(s_i)$. This is exactly the Karhunen–Loëve eigendecomposition of Brownian motion on $[0, 1]$ with covariance kernel $\min(s, t)$.

C Truncated HA kernel

Expanding the definition of $H_{\leq m}$ gives

$$\begin{aligned} K_{\leq m}(x, x') &= \sum_{i=1}^n \sum_{\substack{s \subseteq [d] \\ 1 \leq |s| \leq m}} \left(\prod_{j \in s} 1\{X_{i,j} \leq x_j\} \right) \left(\prod_{j \in s} 1\{X_{i,j} \leq x'_j\} \right) \\ &\stackrel{(a)}{=} \sum_{i=1}^n \sum_{\substack{s \subseteq [d] \\ 1 \leq |s| \leq m}} \prod_{j \in s} 1\{X_{i,j} \leq (x \wedge x')_j\}, \end{aligned}$$

where (a) follows from the identity

$$1\{X_{i,j} \leq x_j\} 1\{X_{i,j} \leq x'_j\} = 1\{X_{i,j} \leq \min(x_j, x'_j)\}.$$

For each i , let

$$s_i(x, x') := \{j \in [d] : X_{i,j} \leq (x \wedge x')_j\}, \quad t_i(x, x') := |s_i(x, x')|.$$

The product $\prod_{j \in s} 1\{X_{i,j} \leq (x \wedge x')_j\}$ equals 1 if and only if $s \subseteq s_i(x, x')$, and equals 0 otherwise. Thus the inner sum counts all subsets of $s_i(x, x')$ of size at most m :

$$K_{\leq m}(x, x') = \sum_{i=1}^n \sum_{\substack{s \subseteq s_i(x, x') \\ 1 \leq |s| \leq m}} 1 = \sum_{i=1}^n \sum_{r=1}^{\min\{m, t_i(x, x')\}} \binom{t_i(x, x')}{r}.$$

D Proof of Theorem 2

i) follows easily from standard ridge regression. By expanding the objective:

$$\frac{1}{2n} \|Y - Z_k \beta\|_2^2 + \frac{\lambda}{2} \|\beta\|_2^2 = \frac{1}{2n} \left(Y^\top Y - 2\beta^\top Z_k^\top Y + \beta^\top Z_k^\top Z_k \beta \right) + \frac{\lambda}{2} \beta^\top \beta.$$

Substituting (4), the first-order condition is

$$-Z_k^\top Y + D_k \beta + n\lambda \beta = 0 \implies (D_k + n\lambda I_k) \beta = Z_k^\top Y.$$

Hence $\hat{\beta}_{k,\lambda}^{\text{PCHAR}} = (D_k + n\lambda I_k)^{-1} Z_k^\top Y = (D_k + n\lambda I_k)^{-1} D_k^{1/2} U_k^\top Y$, and $\hat{f} = Z_k \hat{\beta}$ yields the fitted-value expression.

ii) According to [Tibshirani, 1996] as well as [Bühlmann and Van De Geer, 2011], using (4), the objective separates:

$$\frac{1}{2n} \|Y - Z_k \beta\|_2^2 + \lambda \|\beta\|_1 = \frac{1}{2n} \sum_{j=1}^n y_i^2 + \sum_{j=1}^k \left\{ \frac{d_j}{2n} \beta_j^2 - \frac{w_j \beta_j}{n} + \lambda |\beta_j| \right\}$$

where $w_j := (Z_k^\top Y)_j$. For each j , we minimize $q_j(\beta_j) := \frac{d_j}{2n} \beta_j^2 - \frac{w_j \beta_j}{n} + \lambda |\beta_j|$. By considering the subgradient KKT condition, the unique minimizer is the soft-threshold of w_j/d_j with threshold $n\lambda/d_j$: $\beta_j^* = S\left(\frac{w_j}{d_j}, \frac{n\lambda}{d_j}\right) = \frac{1}{d_j} S(w_j, n\lambda) = \frac{1}{d_j} \text{sign}(w_j) (|w_j| - n\lambda)_+$. Stacking the coordinates yields for $j = 1, \dots, k$,

$$\hat{\beta}_{k,\lambda,j}^{\text{PCHAL}} := \frac{1}{d_j} S(w_j, n\lambda) = \frac{1}{d_j} \text{sign}(w_j) (|w_j| - n\lambda)_+,$$

E Centering the HA design

Principal component analysis is fundamentally applied to centered data. In our setting, the design matrix $H \in \mathbb{R}^{n \times p}$ contains step-function basis evaluations that are generally non-zero-mean. If PCA is applied directly to H , the first principal component will be dominated by the mean level of the basis dictionary rather than by variation around the mean. To remove this artificial location effect, it is standard to *center* the columns of H :

$$\tilde{H} := H - \mathbf{1}_n \mu^\top, \quad \mu := \frac{1}{n} H^\top \mathbf{1}_n,$$

where $\mathbf{1}_n \in \mathbb{R}^n$ denotes the vector of ones. Thus, μ_j is the empirical mean of the j -th basis function across the sample, and every column of \tilde{H} has mean zero. Define the centering matrix

$$J := I_n - \frac{1}{n} \mathbf{1}_n \mathbf{1}_n^\top.$$

A direct computation shows

$$\tilde{H} = JH, \quad \text{and} \quad \tilde{H} \tilde{H}^\top = JHH^\top J.$$

Therefore, centering the columns of H corresponds to double-centering the kernel matrix $K = HH^\top$:

$$\tilde{K} := \tilde{H} \tilde{H}^\top = JKJ.$$

This identity will be used repeatedly when constructing the PC-HA embedding, allowing us to diagonalize $\tilde{H}\tilde{H}^\top$ without explicitly forming the centered design matrix \tilde{H} .

We now show how centering forces the left singular vectors to have mean zero. Suppose \tilde{H} admits the singular value decomposition

$$\tilde{H} = U\sqrt{D}V^\top,$$

where $U \in \mathbb{R}^{n \times n}$ has orthonormal columns and \sqrt{D} is diagonal with nonnegative entries. We have

$$\tilde{H}^\top \mathbf{1}_n = 0 \implies V\sqrt{D}U^\top \mathbf{1}_n = 0.$$

On the subspace corresponding to nonzero singular values, \sqrt{D} and V are invertible, so this implies

$$U^\top \mathbf{1}_n = 0$$

on that subspace. Hence each left singular vector associated with a nonzero singular value has empirical mean zero. Consequently, every column of the PC score matrix

$$Z_k = U_k D_k^{1/2}$$

also has mean zero, since it is a scalar multiple of a mean-zero column of U_k .

To make the role of centering explicit, consider the standard univariate linear regression model (modulo residuals for ease of notation) with an intercept:

$$Y_i = \beta_0 + \beta_1 Z_i, \quad i = 1, \dots, n.$$

Assume that the predictor has already been centered, i.e. its empirical mean is zero:

$$\frac{1}{n} \sum_{i=1}^n Z_i = 0.$$

Let $\bar{Y} := \frac{1}{n} \sum_{i=1}^n Y_i$ denote the empirical mean of the response, and define the centered response

$$\tilde{Y}_i := Y_i - \bar{Y}, \quad i = 1, \dots, n.$$

Taking the empirical mean of both sides of the model gives

$$\bar{Y} = \beta_0 + \beta_1 \cdot \underbrace{\frac{1}{n} \sum_{i=1}^n Z_i}_{=0} = \beta_0.$$

Thus, the intercept is precisely the mean of Y :

$$\beta_0 = \bar{Y}.$$

Substituting $Y_i = \tilde{Y}_i + \bar{Y}$ into the original model,

$$\tilde{Y}_i + \bar{Y} = \beta_0 + \beta_1 Z_i.$$

Since $\beta_0 = \bar{Y}$, these terms cancel, leaving

$$\tilde{Y}_i = \beta_1 Z_i.$$

Hence the centered model is

$$\tilde{Y} = \beta_1 Z,$$

with no intercept term. The effect of centering is therefore to absorb β_0 into the mean of Y .

Importantly, this shows that when a predictor has mean zero, estimating β_1 by regressing \tilde{Y} on Z *without* an intercept yields the same slope coefficient as the original regression of Y on Z *with* an intercept. If one wishes to recover the intercept afterward, it is simply

$$\hat{\beta}_0 = \bar{Y}.$$

This univariate example illustrates the general multivariate principle used in our construction: once the design matrix is column-centered, the intercept in the linear model is fully determined by the mean of the response and does not need to be explicitly included in the regression. This simplification is particularly convenient when working with principal components, since the PC score matrix $Z_k = U_k D_k^{1/2}$ inherits the mean-zero property of U_k .

References

[Aistleitner and Dick, 2014] Aistleitner, C. and Dick, J. (2014). Functions of bounded variation, signed measures, and a general koksma-hlawka inequality. *arXiv preprint arXiv:1406.0230*.

[Benkeser and van der Laan, 2016] Benkeser, D. and van der Laan, M. (2016). The highly adaptive lasso estimator. In *2016 IEEE international conference on data science and advanced analytics (DSAA)*, pages 689–696. IEEE.

[Bibaut and van der Laan, 2019] Bibaut, A. F. and van der Laan, M. J. (2019). Fast rates for empirical risk minimization over cadlag functions with bounded sectional variation norm. *arXiv preprint arXiv:1907.09244*.

[Bickel et al., 1993] Bickel, P. J., Klaassen, C. A. J., Ritov, Y., and Wellner, J. A. (1993). *Efficient and Adaptive Estimation for Semiparametric Models*. Johns Hopkins University Press.

[Bogachev and Ruas, 2007] Bogachev, V. I. and Ruas, M. A. S. (2007). *Measure theory*, volume 1. Springer.

[Breiman et al., 1984] Breiman, L., Friedman, J. H., Olshen, R. A., and Stone, C. J. (1984). *Classification and Regression Trees*. Wadsworth.

[Bühlmann and Van De Geer, 2011] Bühlmann, P. and Van De Geer, S. (2011). *Statistics for high-dimensional data: methods, theory and applications*. Springer Science & Business Media.

[Bühlmann and Yu, 2003] Bühlmann, P. and Yu, B. (2003). Boosting with the l_2 loss: Regression and classification. *Journal of the American Statistical Association*, 98(462):324–339.

[Chernozhukov et al., 2018] Chernozhukov, V., Chetverikov, D., Demirer, M., Duflo, E., Hansen, C., Newey, W., and Robins, J. (2018). Double/debiased machine learning for treatment and structural parameters. *The Econometrics Journal*, 21(1):C1–C68.

[Donoho and Johnstone, 1994] Donoho, D. L. and Johnstone, I. M. (1994). Ideal spatial adaptation by wavelet shrinkage. *Biometrika*, 81(3):425–455.

[Dua et al., 2017] Dua, D., Graff, C., et al. (2017). Uci machine learning repository, 2017. *URL* <http://archive.ics.uci.edu/ml>, 7(1):62.

[Dudoit and van der Laan, 2005] Dudoit, S. and van der Laan, M. J. (2005). Asymptotics of cross-validated risk estimation in estimator selection and performance assessment. *Statistical methodology*, 2(2):131–154.

[Eilers and Marx, 1996] Eilers, P. H. and Marx, B. D. (1996). Flexible smoothing with b-splines and penalties. *Statistical science*, 11(2):89–121.

[Fang et al., 2021a] Fang, B., Guntuboyina, A., and Sen, B. (2021a). Multivariate extensions of isotonic regression and total variation denoising via entire monotonicity and hardy–krause variation. *The Annals of Statistics*, 49(2):769–792.

[Fang et al., 2021b] Fang, B., Guntuboyina, A., and Sen, B. (2021b). Multivariate extensions of isotonic regression and total variation denoising via entire monotonicity and hardy–krause variation.

[Friedman et al., 2010] Friedman, J., Hastie, T., and Tibshirani, R. (2010). Regularization paths for generalized linear models via coordinate descent. *Journal of Statistical Software*, 33(1):1–22.

[Friedman, 1991] Friedman, J. H. (1991). Multivariate adaptive regression splines. *The Annals of Statistics*, 19(1):1–67.

[Gill et al., 1995] Gill, R. D., Laan, M. J., and Wellner, J. A. (1995). Inefficient estimators of the bivariate survival function for three models. In *Annales de l’IHP Probabilités et statistiques*, volume 31, pages 545–597.

[Green and Silverman, 1994] Green, P. J. and Silverman, B. W. (1994). *Nonparametric Regression and Generalized Linear Models: A Roughness Penalty Approach*. Chapman & Hall.

[Györfi et al., 2002] Györfi, L., Kohler, M., Krzyżak, A., and Walk, H. (2002). *A Distribution-Free Theory of Nonparametric Regression*. Springer.

[Halko et al., 2011] Halko, N., Martinsson, P.-G., and Tropp, J. A. (2011). Finding structure with randomness: Probabilistic algorithms for constructing approximate matrix decompositions. *SIAM Review*, 53(2):217–288.

[Hastie et al., 2009] Hastie, T., Tibshirani, R., and Friedman, J. (2009). *The Elements of Statistical Learning: Data Mining, Inference, and Prediction*. Springer, 2 edition.

[Hoerl and Kennard, 1970] Hoerl, A. E. and Kennard, R. W. (1970). Ridge regression: Biased estimation for nonorthogonal problems. *Technometrics*, 12(1):55–67.

[Kim et al., 2009] Kim, S.-J., Koh, K., Boyd, S., and Gorinevsky, D. (2009). ℓ_1 trend filtering. *SIAM Review*, 51(2):339–360.

[Leonov, 1996] Leonov, A. S. (1996). On the total variation for functions of several variables and a multidimensional analog of helly's selection principle. *Mathematical Notes*, 63:61–71.

[Mammen and van de Geer, 1997] Mammen, E. and van de Geer, S. (1997). Locally adaptive regression splines. *The Annals of Statistics*, 25(1):387–413.

[Neuhaus, 1971] Neuhaus, G. (1971). On weak convergence of stochastic processes with multidimensional time parameter. *The Annals of Mathematical Statistics*, 42(4):1285–1295.

[Owen, 2005] Owen, A. B. (2005). Multidimensional variation for quasi-monte carlo. In *International Conference on Statistics in honour of Professor Kai-Tai Fang's 65th birthday*, pages 49–74. World Scientific.

[Robins and Rotnitzky, 1995] Robins, J. M. and Rotnitzky, A. (1995). Semiparametric efficiency in multivariate regression models with missing data. *Journal of the American Statistical Association*, 90(429):122–129.

[Robins et al., 1994] Robins, J. M., Rotnitzky, A., and Zhao, L. P. (1994). Estimation of regression coefficients when some regressors are not always observed. *Journal of the American Statistical Association*, 89(427):846–866.

[Robins et al., 1995] Robins, J. M., Rotnitzky, A., and Zhao, L. P. (1995). Analysis of semiparametric regression models for repeated outcomes in the presence of missing data. *Journal of the American Statistical Association*, 90(429):106–121.

[Rudin et al., 1992] Rudin, L. I., Osher, S., and Fatemi, E. (1992). Nonlinear total variation based noise removal algorithms. *Physica D: Nonlinear Phenomena*, 60(1–4):259–268.

[Schölkopf et al., 1998] Schölkopf, B., Smola, A., and Müller, K.-R. (1998). Nonlinear component analysis as a kernel eigenvalue problem. *Neural Computation*, 10(5):1299–1319.

[Schölkopf and Smola, 2002] Schölkopf, B. and Smola, A. J. (2002). *Learning with Kernels: Support Vector Machines, Regularization, Optimization, and Beyond*. MIT Press.

[Schuler et al., 2024] Schuler, A., Hagemeister, A., and van der Laan, M. (2024). Highly adaptive ridge.

[Sherman and Morrison, 1950] Sherman, J. and Morrison, W. J. (1950). Adjustment of an inverse matrix corresponding to a change in one element of a given matrix. *The Annals of Mathematical Statistics*, 21(1):124–127.

[Stone, 1982] Stone, C. J. (1982). Optimal global rates of convergence for nonparametric regression. *The Annals of Statistics*, 10(4):1040–1053.

[Tibshirani, 1996] Tibshirani, R. (1996). Regression shrinkage and selection via the lasso. *Journal of the Royal Statistical Society Series B: Statistical Methodology*, 58(1):267–288.

[Tibshirani et al., 2005] Tibshirani, R., Saunders, M., Rosset, S., Zhu, J., and Knight, K. (2005). Sparsity and smoothness via the fused lasso. *Journal of the Royal Statistical Society: Series B*, 67(1):91–108.

[Tibshirani, 2014] Tibshirani, R. J. (2014). Adaptive piecewise polynomial estimation via trend filtering. *The Annals of Statistics*, 42(1):285–323.

[Trench, 1999] Trench, W. F. (1999). Eigenvalues and eigenvectors of two symmetric matrices. *IMAGE Bull. Internat. Linear Algebra Soc.*, (22):28–29.

[Tsiatis, 2006] Tsiatis, A. A. (2006). *Semiparametric Theory and Missing Data*. Springer.

[van der Laan, 2017] van der Laan, M. (2017). A generally efficient targeted minimum loss based estimator based on the highly adaptive lasso. *The international journal of biostatistics*, 13(2):20150097.

[van der Laan, 2023] van der Laan, M. (2023). Higher order spline highly adaptive lasso estimators of functional parameters: Pointwise asymptotic normality and uniform convergence rates. *arXiv preprint arXiv:2301.13354*.

[van der Laan et al., 2006] van der Laan, M. J., Dudoit, S., and van der Vaart, A. W. (2006). The cross-validated adaptive epsilon-net estimator. *Annals of Statistics*.

[van der Laan and Rose, 2011] van der Laan, M. J. and Rose, S. (2011). *Targeted Learning: Causal Inference for Observational and Experimental Data*. Springer.

[Van der Laan and Rose, 2018] Van der Laan, M. J. and Rose, S. (2018). *Targeted learning in data science*. Springer.

[van der Laan and Rubin, 2006] van der Laan, M. J. and Rubin, D. (2006). Targeted maximum likelihood learning. *International Journal of Biostatistics*, 2(1).

[van der Vaart, 1998] van der Vaart, A. W. (1998). *Asymptotic Statistics*. Cambridge University Press.

[Wahba, 1990] Wahba, G. (1990). *Spline models for observational data*. SIAM.

[Williams and Seeger, 2001] Williams, C. K. I. and Seeger, M. (2001). Using the nyström method to speed up kernel machines. In *Advances in Neural Information Processing Systems*.

[Wong and Shen, 1995] Wong, W. H. and Shen, X. (1995). Probability Inequalities for Likelihood Ratios and Convergence Rates of Sieve MLES. *The Annals of Statistics*, 23(2):339 – 362.

[Woodbury, 1950] Woodbury, M. A. (1950). Inverting modified matrices. Memorandum report, Statistical Research Group, Princeton University.

[Yeh, 2006] Yeh, J. (2006). *Real analysis: theory of measure and integration second edition*. World Scientific Publishing Company.